
**International Global Navigation Satellite Systems Society**
**IGNSS Symposium 2007**

The University of New South Wales, Sydney, Australia
4 – 6 December, 2007

# Multipath Fading Mitigation

***Andreas Schmid***
Infineon Technologies AG Germany
Phone: +49 203 7298 254, Email: Andreas.Schmid@infineon.com

## ABSTRACT

Satellite navigation is becoming increasingly important for location based services and emergency caller location. Both applications require positioning in urban and indoor areas, where obstacles give rise to reflections, diffraction, and scattering. These obstacles are often near the receiver and lead to multipath signal propagation. Measurement campaigns in urban environments have shown that most multipath components are within an excess delay of less than 500 ns, which corresponds to an excess distance of 150 m. Multiple signal echoes therefore combine with a sub-chip distance at the receiver antenna. Depending on their phase offset, they cause constructive or destructive interference. This then leads to a widely varying amplitude of the combined multipath signal. The resulting fading process degrades the receiver performance. This paper presents a multipath fading mitigation technique that reduces the negative impact of the fading process by adaptively adjusting the detection threshold. The optimal detection threshold is thereby estimated on-the-fly for an unknown fading channel. In relevant environments for mobile phone positioning, the power distribution of the received signal can be modelled with a Rice distribution. The presented technique performs well on a wide range of different Rice factors. The optimal detection threshold is lower for signals with a high Rice factor. A relevant multipath proportion leads to a low Rice factor and the optimal detection threshold is set at a higher level to prevent excessive false detection. If the detection threshold for a line-of-sight signal was applied to a strongly fading signal, false detection would frequently occur. The adaptive detection threshold technique therefore automatically calculates the optimal detection threshold for any Rice factor of the propagation channel.

**KEYWORDS**: Multipath, Fading, Rice, Detection, Threshold.

## 1. INTRODUCTION

Many emerging applications of satellite navigation require positioning in deep urban and moderate indoor environments. The problem is that in these environments the satellite signals do not always reach the receiver in a direct line-of-sight transmission. Instead, there are multiple obstacles surrounding the transmission path, causing reflection, diffraction and scattering. The individual signals superimpose at the receiver antenna. Since most of these obstacles are close to the receiver, their path difference is mostly below 150 m. Measurement campaigns have confirmed that most multipath components have an excess delay of below 500 ns (Pérez-Fontán *et al.* 2004), (Steingass and Lehner 2004), (Jahn *et al.* 1995). Since this delay is less than a chip length, the line-of-sight and multipath components are highly correlated, leading to constructive or destructive interference, depending on the actual excess delay. The movement of the transmitting satellites, receivers and some obstacles form a dynamically varying multipath environment where constructive and destructive interference alternate over time. This characteristic constitutes a multipath fading channel (Krasner *et al.* 2002), (Lehner and Steingass 2005), (Ercek *et al.* 2005). The resulting fading process degrades the receiver performance. While receivers are becoming increasingly sensitive in order to detect strongly attenuated signals, the detection threshold has to be lowered with the reduced signal power. As will be shown subsequently, this causes problems when the received signal is subject to multipath fading. The false alarm rate may increase to an unacceptably high level if the threshold is simply determined based on the line-of-sight signal power. It is also shown in this paper that the negative impact of the fading process can be reduced by adaptively adjusting the detection threshold with the presented multipath fading mitigation method.

## 2. SIGNAL MODEL

Figure 1 provides an overview of the signal processing in the receiver with multipath fading mitigation. In many publications, the received Galileo/GPS signal is expressed in its complex-valued, low-pass equivalent form as (Schmid and Neubauer 2004/2), (Spilker and Parkinson 1996)

$$r_\nu = \sqrt{2\,C}\, d_{\lfloor(\nu\,T_\mathrm{s}+\tau)/T_\mathrm{d}\rfloor}\, c_{\lfloor(\nu\,T_\mathrm{s}+\tau)/T_\mathrm{c}\rfloor}\, \mathrm{e}^{\mathrm{j}\,[2\,\pi\,f_\mathrm{d}\,(\nu\,T_\mathrm{s}+\tau)+\varphi_\mathrm{c}]} + n_\nu \;, \tag{1}$$

where $C$ denotes the received line-of-sight carrier power, $d_{\lfloor(\nu\,T_\mathrm{s}+\tau)/T_\mathrm{d}\rfloor}$ the navigation data, $c_{\lfloor(\nu\,T_\mathrm{s}+\tau)/T_\mathrm{c}\rfloor}$ the spreading code, $f_\mathrm{d}$ the residual frequency deviation after down-conversion, $T_\mathrm{s}$ the sample period, and $n_\nu$ the additive noise component. This signal representation incorporates additive noise, which is typically modelled as zero-mean white GAUSSIAN noise with the variance

$$\sigma_n^2 = \mathrm{E}\big\{|n|^2\big\} = 2\,\mathrm{E}\big\{\Re\{n\}^2\big\} = 2\,\mathrm{E}\big\{\Im\{n\}^2\big\} = 2\,\mathcal{N}_0\,B\,F \;, \tag{2}$$

where $\mathrm{E}\{\,\cdot\,\}$ is the operator for the expectation value,

$$\mathcal{N}_0 = k\,T_0 \tag{3}$$

denotes the noise Power Spectral Density (PSD), $B$ the noise bandwidth, $F$ the front-end noise figure, $k = 1.381\times10^{-23}\,\mathrm{W\,s/K}$ the BOLTZMAN constant, and $T_0$ the noise temperature (Spilker and Parkinson 1996). The real and imaginary part of $n_\nu$ are uncorrelated

$$\mathrm{E}\{\Re\{n\}\,\Im\{n\}\} = 0 \;. \tag{4}$$

The noise temperature $T_0 = 290\,\mathrm{K}$ and the front-end noise figure $F = 3\,\mathrm{dB}$ are applied for all subsequent simulations as they are typical values used in literature.

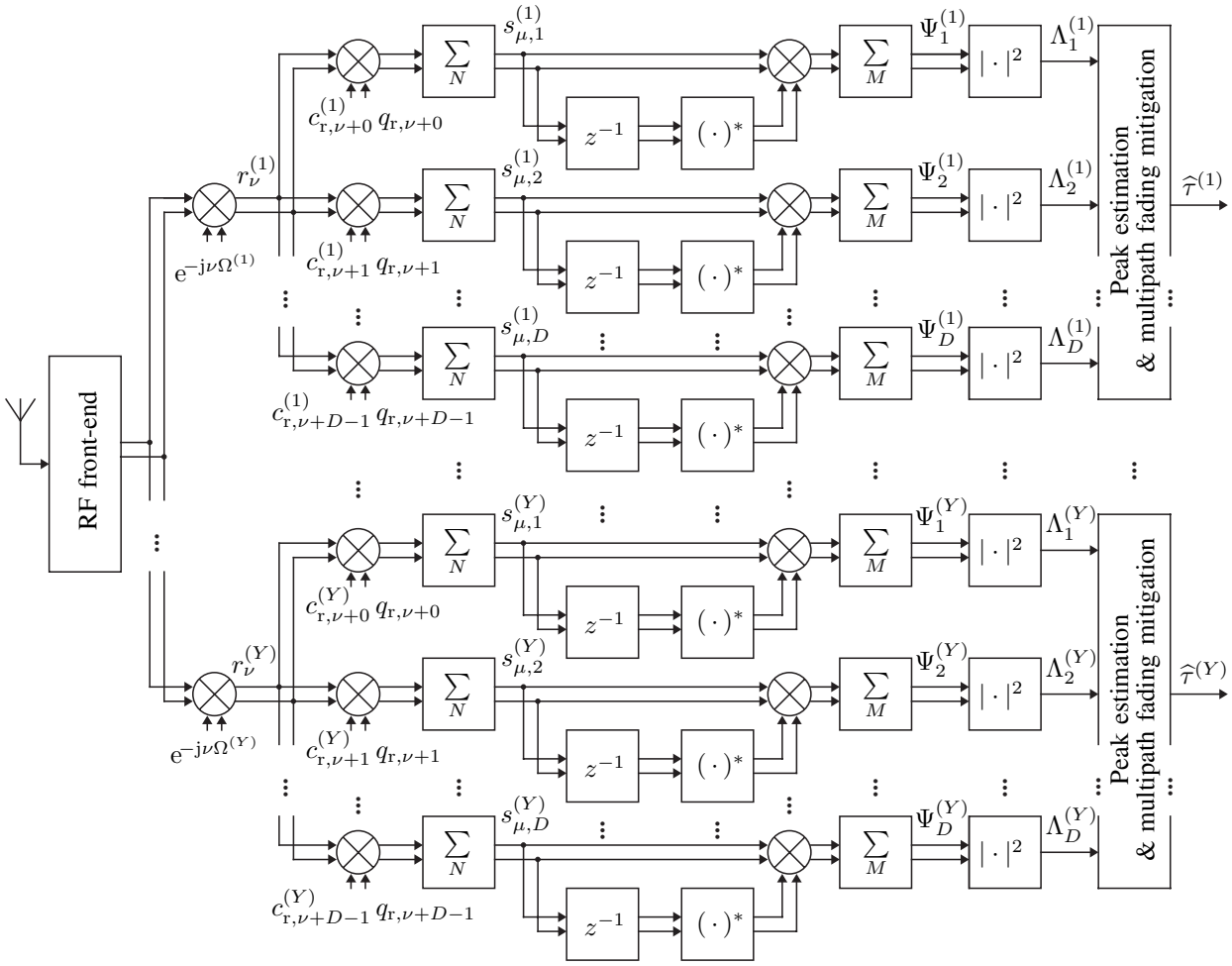


Figure 1. Highly parallel reception with multipath fading mitigation.

However, obstructions in deep urban areas and indoor environments cause reflections, diffraction and scattering. This gives rise to multipath signal propagation with different versions of the signal arriving at the receiver at different times. The multipath signals are combined at the receiver antenna by superposition. Depending on their phase offset, this causes constructive or destructive interference (Schmid and Neubauer 2004/1). In an environment where the satellite transmitter, the receiver and even some of the obstacles are in motion, this leads to a multipath fading process (Krasner *et al.* 2002), (Lehner and Steingass 2005), (Ercek *et al.* 2005). To model a fading Galileo/GPS signal, its definition in (1) is modified to

$$r_\nu = \sqrt{2\,C}\, c_{\lfloor(\nu\,T_\mathrm{s}+\tau)/T_\mathrm{c}\rfloor}\, q_{\lfloor(\nu\,T_\mathrm{s}+\tau)/T_\mathrm{c}\rfloor}\, \mathrm{e}^{\mathrm{j}\,(2\,\pi\,f_\mathrm{d}\,\nu\,T_\mathrm{s}+\varphi_\mathrm{c})}\, \theta_\nu + n_\nu \;, \tag{5}$$

where $\theta_\nu$ describes the fading characteristic. The fading variable $\theta$ has the mean magnitude

$$|m_\theta| = |\mathrm{E}\{\theta\}| = 1 \;. \tag{6}$$

GPS receivers typically employ the NEYMAN-PEARSON detection criterion, where the false detection probability $P_\mathrm{f}$ must not exceed a fixed number (Van Dierendonck 1996). Then for the given false detection probability, the probability of detection $P_\mathrm{d}$ is maximized. The detection threshold $\lambda$ is therefore chosen as low as possible, without exceeding the maximum false

detection probability (Schmid and Neubauer 2005), (Schmid 2007). False detection is caused by out-of-phase correlation and additive noise. The multipath fading modifies both the correlation peak and the out-of-phase autocorrelation values. If the detection threshold is not adjusted, the fading correlation peak changes the probability of detection. At the same time, the fading out-of-phase autocorrelation values lead to a changed false detection probability, which differs from the admissible level. The multipath fading mitigation method of this paper therefore estimates the correlation variance and mean magnitude. This allows optimal adjustment of the detection threshold to the fading characteristic of the Galileo/GPS signal. The false detection probability is kept at the selected level and the probability of detection is maximized. The knowledge of the fading characteristic can thus be used to recover a large portion of the receiver performance.

The RICE distribution is frequently used to model multipath fading in urban and indoor environments (Krasner *et al.* 2002), (Lehner and Steingass 2005), (Ercek *et al.* 2005). The magnitude of a complex-valued GAUSSIAN distributed variable $\theta$ with the expectation value

$$m_\theta = \mathrm{E}\{\theta\} \; , \tag{7}$$

and the combined real and complex variance

$$\sigma_\theta^2 = \mathrm{E}\big\{|\theta - m_\theta|^2\big\} \tag{8}$$

obeys the RICE distribution (Proakis 2001)

$$p_{|\theta|}(\alpha) = \begin{cases} \frac{2\,\alpha}{\sigma_\theta^2} \exp\!\Big(-\frac{\alpha^2+|m_\theta|^2}{\sigma_\theta^2}\Big)\; \mathrm{I}_0\!\Big(\frac{2\,|m_\theta|\,\alpha}{\sigma_\theta^2}\Big) \; , & \alpha \geqslant 0 \\ 0 \; , & \text{else} \; , \end{cases} \tag{9}$$

with

$$\alpha = |\theta| \; . \tag{10}$$

The modified BESSEL function of first kind and zero order is denoted by $\mathrm{I}_0(\cdot)$. The fading signal is thereby characterized by the RICE factor

$$\mathcal{K} = \frac{|m_\theta|^2}{\sigma_\theta^2} \; . \tag{11}$$

The line-of-sight signal is superimposed by multiple time-varying reflections, which form the fading process around the line-of-sight signal. The variance of the fading variable

$$\sigma_\theta^2 = \mathrm{E}\big\{|\theta - m_\theta|^2\big\} = \frac{1}{\mathcal{K}} \tag{12}$$

follows from (11) and (6).

## 3. FADING ADAPTATION

The next step in the signal processing flow of Figure 1 is the coherent integration of $N$ samples. It is subsequently assumed that the coherent integration interval $N\,T_\mathrm{s}$ is chosen so as to be no longer than the coherence time of the multipath propagation channel, such that the fading variable $\theta_\nu$ can be approximated to be constant during each coherent integration interval. By making the additional assumption that the fading variable is uncorrelated between integration

intervals, the derivation traceability improves. The coherently integrated predetection result can be derived as (Schmid and Neubauer 2004/2), (Schmid 2007)

$$\begin{aligned} s_\mu &= \sum_{\nu=\mu\,N}^{(\mu+1)\,N-1} r_\nu\, c_{\lfloor(\nu\,T_\mathrm{s}+\widehat{\tau})/T_\mathrm{c}\rfloor} \\ &\simeq \sqrt{2\,C}\,R(\tau-\widehat{\tau})\,\mathrm{sinc}(f_\mathrm{d}\,N\,T_\mathrm{s})\,\mathrm{e}^{\mathrm{j}\,[(2\,\mu+1)\,\pi\,f_\mathrm{d}\,N\,T_\mathrm{s}+\varphi_\mathrm{c}]}\,\theta_{N\mu}+w_\mu\ , \end{aligned} \tag{13}$$

where $c_{\lfloor(\nu\,T_\mathrm{s}+\widehat{\tau})/T_\mathrm{c}\rfloor}$ denotes the replica despreading code, $R(\,\cdot\,)$ the correlation function, $\tau$ the received code phase, $\widehat{\tau}$ the despreading code phase, and $w_\mu$ the zero-mean white GAUSSIAN noise component with the variance

$$\sigma_w^2=\mathrm{E}\{|w|^2\}=2\,\mathrm{E}\{\Re\{w\}^2\}=2\,\mathrm{E}\{\Im\{w\}^2\}=N\,\sigma_n^2=2\,Nk\,T_0\,B\,F\ . \tag{14}$$

The GAUSSIAN variables $\theta_{N\mu}$ and $w_\mu$ in (13) lead to a GAUSSIAN distributed variable $s_\mu$ with the mean

$$m_{s_\mu}=\mathrm{E}\{s_\mu\}=\sqrt{2\,C}\,R(\tau-\widehat{\tau})\,\mathrm{sinc}(f_\mathrm{d}\,N\,T_\mathrm{s})\,\mathrm{e}^{\mathrm{j}\,[(2\,\mu+1)\,\pi\,f_\mathrm{d}\,N\,T_\mathrm{s}+\varphi_\mathrm{c}]}\,m_\theta \tag{15}$$

and the variance

$$\sigma_{s_\mu}^2=\mathrm{E}\{|s_\mu-\mathrm{E}\{s_\mu\}|^2\}=2\,C\,R^2(\tau-\widehat{\tau})\,\mathrm{sinc}^2(f_\mathrm{d}\,N\,T_\mathrm{s})\,\sigma_\theta^2+\sigma_w^2\ . \tag{16}$$

The differential correlation result is calculated as

$$\Psi=\sum_{\mu=1}^{M-1} s_\mu\,s_{\mu-1}^*\ . \tag{17}$$

With the results in (Schmid and Neubauer 2004/2) and (Schmid 2007), its expectation value can be derived as

$$\begin{aligned} m_\Psi &= \mathrm{E}\{\Psi\}=(M-1)\,m_{s_\mu}\,m_{s_{\mu-1}}^* \\ &= 2\,(M-1)\,C\,R^2(\tau-\widehat{\tau})\,\mathrm{sinc}^2(f_\mathrm{d}\,N\,T_\mathrm{s})\,\mathrm{e}^{\mathrm{j}\,2\,\pi\,f_\mathrm{d}\,N\,T_\mathrm{s}}\ . \end{aligned} \tag{18}$$

Incorporating the results from (Schmid and Neubauer 2004/2) and (Schmid 2007), the correlation variance for the RICE fading channel is derived as

$$\boxed{\begin{aligned} \sigma_\Psi^2 &= \mathrm{E}\{|\Psi-\mathrm{E}\{\Psi\}|^2\}=(M-1)\left(\sigma_{s_\mu}^4+2\,\sigma_{s_\mu}^2\,|m_{s_\mu}|^2\right) \\ &= (M-1)\left[\sigma_w^4+4\,C^2\,R^4(\tau-\widehat{\tau})\,\mathrm{sinc}^4(f_\mathrm{d}\,N\,T_\mathrm{s})\,\frac{2\,\mathcal{K}+1}{\mathcal{K}^2}\right. \\ &\qquad \left.+\,4\,C\,\sigma_w^2\,R^2(\tau-\widehat{\tau})\,\mathrm{sinc}^2(f_\mathrm{d}\,N\,T_\mathrm{s})\,\frac{\mathcal{K}+1}{\mathcal{K}}\right]\ . \end{aligned}} \tag{19}$$

## 4. MULTIPATH FADING MITIGATION

The last step is correlation peak estimation and multipath fading mitigation. The estimation of the unknown code phase $\tau$ is best accomplished by maximizing the magnitude or squared magnitude of the differential correlation result (Proakis 2001)

$$\Lambda=|\Psi|^2=\Re\{\Psi\}^2+\Im\{\Psi\}^2\ . \tag{20}$$

The detection test statistic $\Lambda$ obeys the noncentral CHI-SQUARED cumulative distribution (Proakis 2001), (Schmid 2007)

$$P_\Lambda(\Lambda) \simeq 1 - \mathrm{Q}_1\left(\sqrt{\frac{2\,|m_\Psi|^2}{\sigma_\Psi^2}},\, \sqrt{\frac{2\Lambda}{\sigma_\Psi^2}}\right). \tag{21}$$

Due to the unknown signal attenuation, it is not reliable to just determine the code phase $\tau$ based on the highest value of $\Lambda$. Instead, the highest value of $\Lambda$ also has to be sufficiently large, such that a correlation peak can be assumed. It is therefore compared to a detection threshold $\lambda$. If $\Lambda$ exceeds the threshold, hypothesis $\mathrm{H}_1$ is assumed

$$\Lambda \underset{\mathrm{H}_0}{\overset{\mathrm{H}_1}{\gtrless}} \lambda\,. \tag{22}$$

Hypothesis $\mathrm{H}_1$ represents the case where the estimated code phase $\widehat{\tau}$ corresponds to the actual code phase $\tau$. Hypothesis $\mathrm{H}_0$ represents the out-of-phase correlation and is assumed if $\Lambda$ does not exceed the threshold.

The detection threshold $\lambda$ of satellite navigation receivers is typically determined with the NEYMAN-PEARSON criterion (Van Dierendonck 1996). It maximizes the probability of detection $P_\mathrm{d}$ for a given false detection probability $P_\mathrm{f}$. The probability of false detection

$$P_\mathrm{f} = \Pr\{\Lambda \geqslant \lambda|\mathrm{H}_0\} = \int_\lambda^\infty p_{\Lambda|\mathrm{H}_0}(\Lambda)\; d\Lambda = 1 - P_{\Lambda|\mathrm{H}_0}(\lambda) = \mathrm{Q}_1\left(\sqrt{\frac{2\,|m_{\Psi,\mathrm{H}_0}|^2}{\sigma_{\Psi,\mathrm{H}_0}^2}},\, \sqrt{\frac{2\,\lambda}{\sigma_{\Psi,\mathrm{H}_0}^2}}\right) \tag{23}$$

with

$$m_{\Psi,\mathrm{H}_0} = m_\Psi\big|_{R^2(\tau-\widehat{\tau})=R_\mathrm{m}^2}\,, \quad \sigma_{\Psi,\mathrm{H}_0}^2 = \sigma_\Psi^2\big|_{R^2(\tau-\widehat{\tau})=R_\mathrm{m}^2} \tag{24}$$

is the probability that the maximum out-of-phase autocorrelation value $R_\mathrm{m}$ leads to false detection (Spilker and Parkinson 1996). With (23), the optimal detection threshold

$$\lambda = P_{\Lambda|\mathrm{H}_0}^{-1}(1 - P_\mathrm{f}) = \frac{\sigma_{\Psi,\mathrm{H}_0}^2}{2}\left[\mathrm{Q}_{1,\beta}^{-1}\left(\sqrt{\frac{2\,|m_{\Psi,\mathrm{H}_0}|^2}{\sigma_{\Psi,\mathrm{H}_0}^2}},\, P_\mathrm{f}\right)\right]^2 \tag{25}$$

equals the inverse cumulative distribution of $\Lambda$ for the false detection hypothesis $P_{\Lambda|\mathrm{H}_0}^{-1}(\cdot)$, which can be obtained with the inverse first-order MARCUM-Q function with respect to its second argument $\mathrm{Q}_{1,\beta}^{-1}(\alpha,\,\gamma)$.

If the detection threshold $\lambda$ is calculated for a line-of-sight signal and then applied to signals received from a RICE multipath fading channel, the resulting probability of false detection $P_\mathrm{f}$ is above the admissible level. Figure 2 shows $P_\mathrm{f}$ as a function of the RICE factor $\mathcal{K}$. The detection threshold $\lambda$ in Figure 2 has been calculated to yield $P_\mathrm{f} = 10^{-5}$ for a non-fading signal. This is the standard approach for state-of-the-art receivers. However, once the RICE factor drops to below 100, the false alarm probability starts to increase. The probability of false alarm is almost a magnitude too large for $\mathcal{K} = 10$. For low RICE factors, the false alarm probability approaches 100 %, which means that false acquisition leading to severe positioning errors is almost guaranteed.

In order for the false detection probability $P_\mathrm{f}$ in (23) to reach the exact permissable level, the detection threshold $\lambda$ in (25) has to be calculated as a function of the actual RICE factor $\mathcal{K}$ of the propagation channel, where $m_{\Psi,\mathrm{H}_0} = m_\Psi|_{R^2(\tau-\widehat{\tau})=R_\mathrm{m}^2}$ is specified in (18) and $\sigma_{\Psi,\mathrm{H}_0}^2 =$

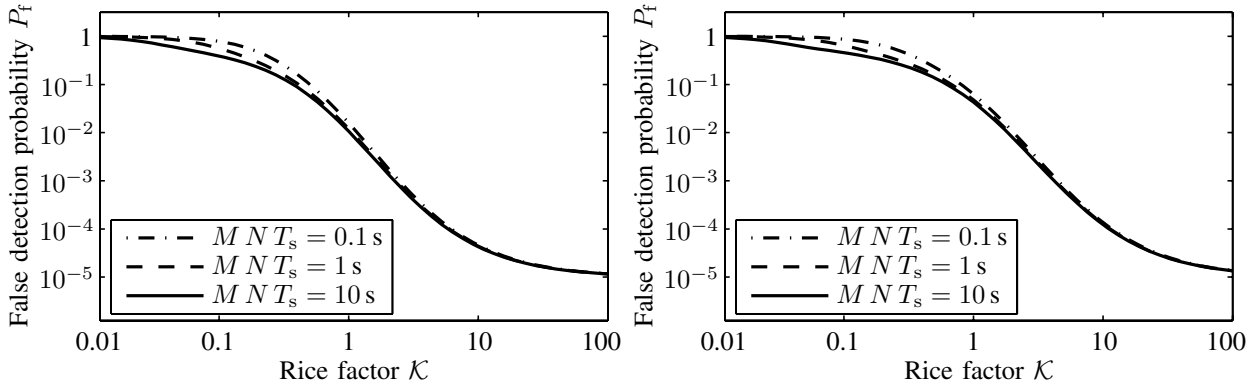


(a) GPS L1-C/A.

(b) Galileo E1-C.

Figure 2. Probability of false detection without threshold adaptation for $T_0 = 290\,\mathrm{K}$, $F = 3\,\mathrm{dB}$, $N\,T_\mathrm{s} = 20\,\mathrm{ms}$, and $C/\mathcal{N}_0 = 45\,\mathrm{dBHz}$.

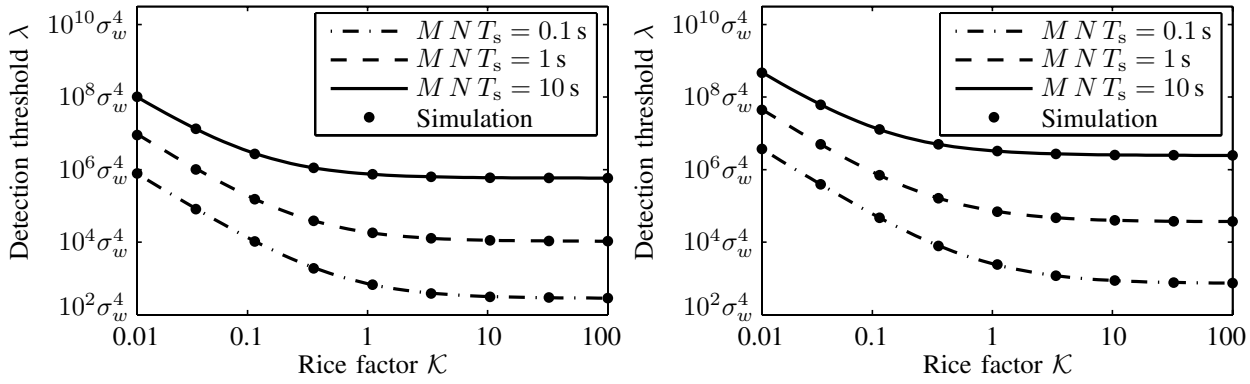


(a) GPS L1-C/A.

(b) Galileo E1-C.

Figure 3. Optimal detection threshold $\lambda$ for RICE fading for $T_0 = 290\,\mathrm{K}$, $F = 3\,\mathrm{dB}$, $N\,T_\mathrm{s} = 20\,\mathrm{ms}$, $C/\mathcal{N}_0 = 45\,\mathrm{dBHz}$, and $B = 4.092\,\mathrm{MHz}$.

$\sigma_\Psi^2|_{R^2(\tau-\widehat{\tau})=R_\mathrm{m}^2}$ is given in (19). A low RICE factor $\mathcal{K}$ requires a high detection threshold $\lambda$ and a high RICE factor requires a low detection threshold. In Figure 3, the optimal detection threshold is presented as a function of the RICE factor. It must be high enough not to lead to a violation of the maximum allowed $P_\mathrm{f}$. Using this threshold will maintain a constant false alarm probability $P_\mathrm{f} = 10^{-5}$ for all possible RICE factors.

The RICE factor can be estimated with different methods (Greenstein *et al.* 1999), (Tepedelenlioglu *et al.* 2003). However, none of them is required here. It is already sufficient to estimate the mean magnitude $|m_\Psi|$ and variance $\sigma_\Psi^2$ of the correlation result $\Psi$. The decision statistic $\Lambda$ is the squared magnitude of the GAUSSIAN distributed differential correlation result $\Psi$. The combination of its first moment

$$\mathrm{E}\{\Lambda\} = \mathrm{E}\{|\Psi|^2\} = |m_\Psi|^2 + \sigma_\Psi^2 \tag{26}$$

with its second moment

$$\mathrm{E}\{\Lambda^2\} = \mathrm{E}\{|\Psi|^4\} = \sigma_\Psi^4 + 2\,\sigma_\Psi^2\,|m_\Psi|^2 + \left(\sigma_\Psi^2 + |m_\Psi|^2\right)^2 \tag{27}$$

yields the relationships

$$|m_\Psi|^2 = \sqrt{2\,\left(\mathrm{E}\{\Lambda\}\right)^2 - \mathrm{E}\{\Lambda^2\}} \tag{28}$$

and

$$\sigma_{\Psi}^2 = \mathrm{E}\{\Lambda\} - |m_{\Psi}|^2 \, . \tag{29}$$

This can be utilized to estimate the parameters $|m_{\Psi,\mathrm{H}_0}|$ and $\sigma_{\Psi,\mathrm{H}_0}^2$. Since both parameters should be estimated for hypothesis $\mathrm{H}_0$, the first step is to exclude the correlation peak. The different decision statistics within one frequency search bin are denoted as $\Lambda_\iota$. The different code phase search bins are thereby indexed with $\iota$. First, the index $\hat{\imath}$, which originates most likely from the correlation peak is selected. The interval of the correlation peak is excluded in the following estimation algorithm, such that only the out-of-phase correlation values are used. The variable $D$ represents the number of code phase search bins. The first moment is hence estimated by

$$\mathcal{M}_1 = \frac{1}{D - 2\left\lceil T_\mathrm{c}/T_\mathrm{s} \right\rceil + 1} \left[ \sum_{\nu=1}^{\hat{\imath}-\lceil T_\mathrm{c}/T_\mathrm{s} \rceil} \Lambda_\nu + \sum_{\nu=\hat{\imath}+\lceil T_\mathrm{c}/T_\mathrm{s} \rceil}^{D} \Lambda_\nu \right] \simeq \mathrm{E}\{\Lambda\} \, \big|_{\tau \neq \hat{\tau}} \tag{30}$$

and the second moment is estimated by

$$\mathcal{M}_2 = \frac{1}{D - 2\left\lceil T_\mathrm{c}/T_\mathrm{s} \right\rceil + 1} \left[ \sum_{\nu=1}^{\hat{\imath}-\lceil T_\mathrm{c}/T_\mathrm{s} \rceil} \Lambda_\nu^2 + \sum_{\nu=\hat{\imath}+\lceil T_\mathrm{c}/T_\mathrm{s} \rceil}^{D} \Lambda_\nu^2 \right] \simeq \mathrm{E}\big\{\Lambda^2\big\} \, \big|_{\tau \neq \hat{\tau}} \, , \tag{31}$$

where $\lceil \cdot \rceil$ is the ceiling function for rounding to the next higher or equal integer.

With (28), the squared magnitude of the differential correlation mean for hypothesis $\mathrm{H}_0$ can be estimated as

$$|\widehat{m}_{\Psi,\mathrm{H}_0}|^2 = \sqrt{2\,\mathcal{M}_1^2 - \mathcal{M}_2} \, . \tag{32}$$

The differential correlation variance for hypothesis $\mathrm{H}_0$ can hence be estimated as

$$\widehat{\sigma}_{\Psi,\mathrm{H}_0}^2 = \mathcal{M}_1 - |\widehat{m}_{\Psi,\mathrm{H}_0}|^2 \, . \tag{33}$$

Incorporating the previous results, the adaptive detection threshold with multipath fading mitigation is

$$\widehat{\lambda} = P_{\Lambda|\mathrm{H}_0}^{-1}(1 - P_\mathrm{f}) = \frac{\widehat{\sigma}_{\Psi,\mathrm{H}_0}^2}{2} \left[ \mathrm{Q}_{1,\beta}^{-1}\left( \sqrt{\frac{2\,|\widehat{m}_{\Psi,\mathrm{H}_0}|^2}{\widehat{\sigma}_{\Psi,\mathrm{H}_0}^2}}, \, P_\mathrm{f} \right) \right]^2 \, . \tag{34}$$

Figure 3 compares the optimal detection threshold for RICE fading channels versus a simulation of the estimated threshold with (32) and (33). The simulation utilizes $1021 \times 4$ different code phase bins for the GPS L1-C/A signal and $4090 \times 4$ code phase bins for the Galileo E1-C signal, due to the front-end bandwidth being four times the chip rate. This corresponds to a simple full epoch code search and works well for the whole range of RICE factors. As can be seen in Figure 3, the detection threshold for fading signals with a low RICE factor is higher than for non-fading signals with a very high RICE factor. The simulated detection thresholds of Figure 3 are furthermore translated into the resulting false detection probabilities in Figure 4. It can be seen that the false alarm probability is kept constant at $P_\mathrm{f} = 10^{-5}$. This is the primary target of the multipath fading mitigation technique. The simulations in Figure 3 and 4 do not make use of any of the approximations in this thesis. They simulate the results for actual white GAUSSIAN noise samples combined with the Galileo/GPS satellite signal at the input of the receiver chain in Figure 1. As can be seen, the simulations match very well with the theoretical derivations. Figure 4 shows that the multipath fading mitigation works effectively. The RICE fading does not increase the probability of false acquisition any more, as previously in Figure 2. The false alarm probability is at the permissable level of $P_\mathrm{f} = 10^{-5}$ for the whole range of different RICE

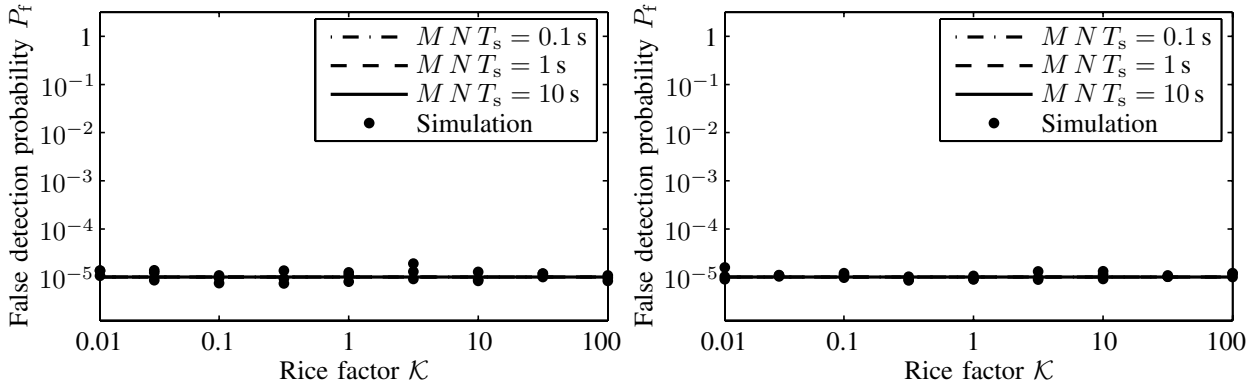


(a) GPS L1-C/A. (b) Galileo E1-C.

Figure 4. Probability of false detection with threshold adaptation for $T_0 = 290\,\mathrm{K}$, $F = 3\,\mathrm{dB}$, $N\,T_\mathrm{s} = 20\,\mathrm{ms}$, and $C/\mathcal{N}_0 = 45\,\mathrm{dBHz}$.

factors.

## 5. RECEPTION SENSITIVITY

Figure 5 shows the reception sensitivity achieved by the optimal detection threshold $\lambda$ of Figure 3. The decision statistic

$$\Lambda = |\Psi|^2 = \left| \sum_{\mu=1}^{M-1} s_\mu \, s_{\mu-1}^* \right|^2 \tag{35}$$

results in the detection probability

$$P_\mathrm{d} = \Pr\{\Lambda \geqslant \lambda | \mathrm{H}_1\} = 1 - P_{\Lambda|\mathrm{H}_1}(\lambda) = \mathrm{Q}_1\left( \sqrt{\frac{2\,|m_{\Psi,\mathrm{H}_1}|^2}{\sigma^2_{\Psi,\mathrm{H}_1}}}, \sqrt{\frac{2\,\lambda}{\sigma^2_{\Psi,\mathrm{H}_1}}} \right) \tag{36}$$

by applying

$$m_{\Psi,\mathrm{H}_1} = m_\Psi\big|_{R^2(\tau-\widehat{\tau})=N^2} \,, \quad \sigma^2_{\Psi,\mathrm{H}_1} = \sigma^2_\Psi\big|_{R^2(\tau-\widehat{\tau})=N^2} \,. \tag{37}$$

The reception sensitivity in Figure 5 corresponds to $P_\mathrm{d} = 90\,\%$. The figure is provided to show how the RICE fading influences the receiver sensitivity. It can be observed that the sensitivity degrades slightly for lower $\mathcal{K}$. However, this effect is barely noticeable since the degradation is really minor. The reason for it is the increase in detection threshold to prevent false acquisition due to fading behavior.

## 6. CONCLUSION

Measurement campaigns confirm that multipath propagation is a serious problem in deep urban and indoor environments. Since the excess delays are relatively short, a multipath fading process arises. If this multipath fading characteristic is incorporated in the calculation of the optimal detection threshold excessively high false alarm rates may be the result. The presented multipath fading mitigation method prevents this by estimating the optimal detection threshold for different fading channels. It performs well on a wide range of different RICE factors. The optimal

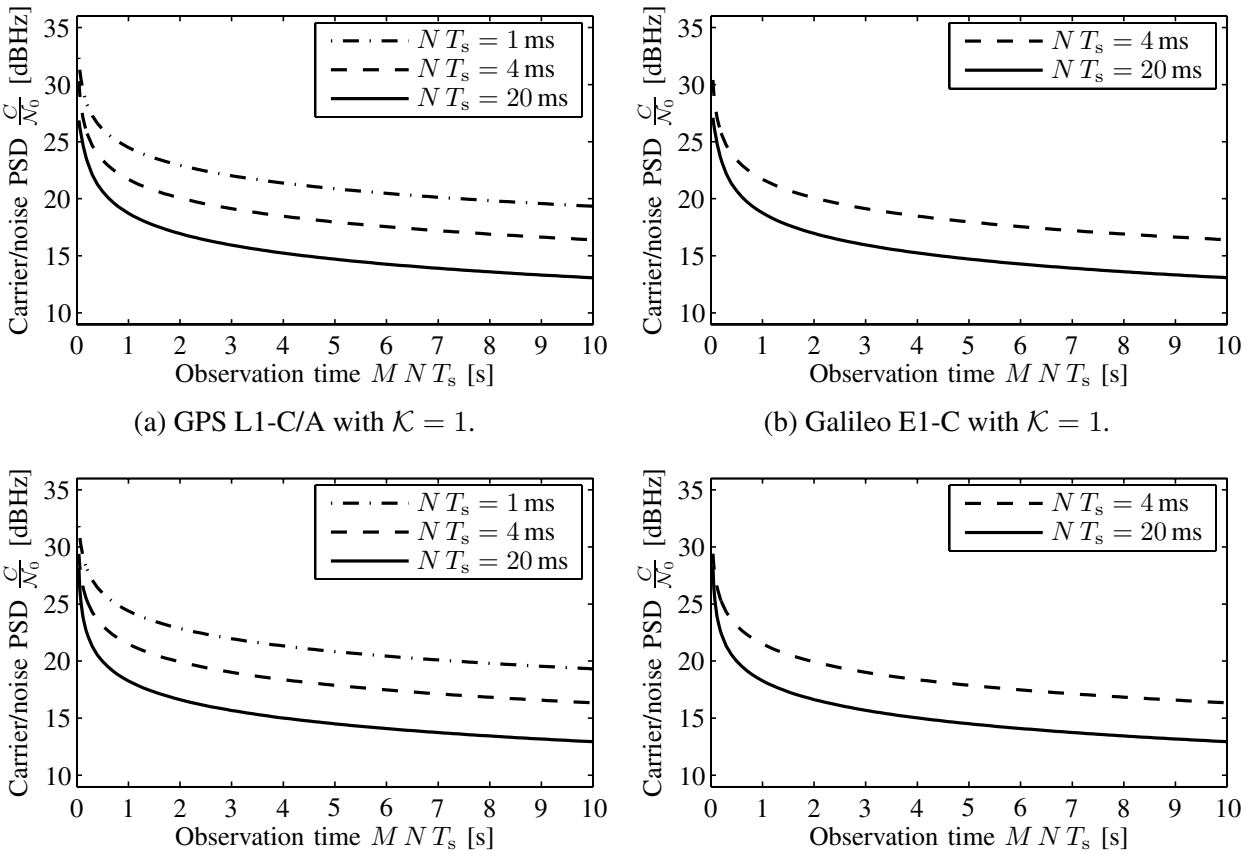


(a) GPS L1-C/A with $\mathcal{K} = 1$.

(b) Galileo E1-C with $\mathcal{K} = 1$.

(c) GPS L1-C/A with $\mathcal{K} = 10$.

(d) Galileo E1-C with $\mathcal{K} = 10$.

Figure 5. Reception sensitivity with the multipath fading mitigation technique for $T_0 = 290\,\mathrm{K}$, $F = 3\,\mathrm{dB}$, $P_\mathrm{f} = 10^{-5}$, and $P_\mathrm{d} = 90\,\%$.

detection threshold is lower for signals with a high RICE factor. A relevant multipath proportion leads to a low RICE factor and the optimal detection threshold is set at a higher level to prevent excessive false detections. If the detection threshold for a line-of-sight signal was applied to a strongly fading signal, false detection would frequently occur. The adaptive detection threshold technique therefore automatically calculates the optimal detection threshold for any RICE factor of the propagation channel. Effectively, the present algorithm calculates the optimal detection threshold for multipath fading signals as well as line-of-sight signals.

## REFERENCES

Ercek R, De Doncker P, Grenez F (2005) Study of pseudo-range error due to non-line-of-sight-multipath in urban canyons, *Proceedings ION GNSS International Technical Meeting of the Satellite Division*, 1083-1094

Greenstein LJ, Michelson DG, Erceg V (1999) Moment-method estimation of the Ricean K-factor, *IEEE Communications Letters* 6(3): 175-176

Jahn A, Buonomo S, Sforza M, Lutz E (1995) Narrow- and wide-band channel characterization for land mobile satellite systems: Experimental results at L-band, *Proceedings of the International Mobile Satellite Conference*, 115-121

Krasner NF, Marshall G, Riley W (2002) Position determination using hybrid GPS/cellphone ranging, *Proceedings of the ION GPS International Technical Meeting of the Satellite Division*, 165-176

Lehner A, Steingass A (2005) A novel channel model for land mobile satellite navigation, *Proceedings of the ION GNSS International Technical Meeting of the Satellite Division*, 2132-2138

Pérez-Fontán F, Sanmartín B, Steingass A, Lehner A, Selva E, Kubista J, Arbesser-Rastburg B (2004) Measurements and modeling of the satellite-to-indoor channel for Galileo, *Proceedings of the European Navigation Conference GNSS*, paper 88

Proakis JG (2001) *Digital Communications* (4th edition), McGraw-Hill, New York, NY, USA

Schmid A, Neubauer A (2004/1) Evaluation of Galileo BOC modulation versus GPS BPSK modulation in multipath propagation scenarios, *Proceedings of the European Radio Navigation Systems and Services*

Schmid A, Neubauer A (2004/2) Performance evaluation of differential correlation for single shot measurement positioning, *Proceedings of the ION GNSS International Technical Meeting of the Satellite Division*, 1998-2009

Schmid A, Neubauer A (2005) Carrier to noise power estimation for enhanced sensitivity Galileo/GPS receivers, *Proceedings of the IEEE Vehicular Technology Spring Conference*

Schmid A (2007) *Enhanced Sensitivity for Galileo and GPS Receivers*, awaiting book publication

Spilker Jr. JJ, Parkinson BW (1996) Chapter 3: GPS Signal Structure and Theoretical Performance, in: Parkinson BW, Spilker Jr. JJ (eds), *Global Positining System: Theory and Applications*, American Institute of Aeronautics and Astronautics, Washington, DC, USA, Vol. 1, 57-119

Steingass A, Lehner A (2004) Measuring the navigation multipath channel - A statistical analysis, *Proceedings of the ION GNSS International Technical Meeting of the Satellite Division*, 1157-1164

Tepedelenlioglu C, Abdi A, Giannakis GB (2003) The Ricean K factor: Estimation and performance analysis, *IEEE Transactions on Wireless Communications* 2(4), 799-819

Van Dierendonck AJ (1996) Chapter 8: GPS Receivers, in: Parkinson BW, Spilker Jr. JJ (eds), *Global Positining System: Theory and Applications*, American Institute of Aeronautics and Astronautics, Washington, DC, USA, Vol. 1, 329-407